International Journal of Applied Mathematics

Volume 38 No. 5s, 2025

ISSN: 1311-1728 (printed version); ISSN: 1314-8060 (on-line version)

A NOVEL APPROACH FOR ORAL CANCER CLASSIFICATION AND SURVIVAL RATE PREDICTION USING ADVANCED DEEP LEARNING APPROACH

[1] A . Subbulakshmi, [2] Dr. S. Sudha

[1]Research Scholar, Computer Application

Hindustan Institute Of Technology And Science

Y2subu@Gmail.Com

[2]Professor, Computer Application

Hindustan Institute Of Technology And Science

Sudhas@Hindustanuniv.Ac.In

Abstract

The rising rate of oral cancers (OC) which is (oral squamous cell carcinoma [OSCC]) more troubling still, the increasing rate of OSCC in younger populations adds significance to the need for valid and consistent prediction methods. More typical research methods for predicting OSCC and cancer in general are usually extremely computationally intensive and have extremely low prediction accuracy. An automated OC classification pipeline that employs deep recurrent spiking neural networks (DRSNN) has been developed. To develop this pipeline, the input was pre-processed by applying a median filter (MF), unsharp masking, and contrast-limited adaptive histogram equalization (CLAHE) to filter some noise and enhance the images. Then features were extracted using the Gabor Wavelet Transform (GWT). After feature extraction, a newly developed Hybrid Bowerbird-Grey Wolf Optimization (HBGWO) was implemented to determine the most representative features. Finally, the images were classified as normal or abnormal using the DRSNN classifier, hence outlining a quicker and efficient prediction methodology for OC detection. The framework was validated using the Kaggle Oral OSCC (lips and tongue images) dataset that was simultaneously augmented to 1,310 samples. According to the experimental data, the suggested method outperforms the F-measure, accuracy, specificity, and precision of the predictive models that have been in use for the past year and achieves an overall classification accuracy of 98.92% when compared favorably to current relevant predictive algorithms, such as ANN, DNN, DCNN-LSTM, and SVM.

Volume 38 No. 5s, 2025

ISSN: 1311-1728 (printed version); ISSN: 1314-8060 (on-line version)

Keywords: *Oral Cancer, Median Filter, Gabor Wavelet Transform, Bowerbird Algorithm, Grey Wolf Algorithm, RSNN.*

1.Introduction

OC is a public health issue dominated by squamous cell carcinoma of the oral cavity. OC is a significant mucin type, with high incidence and mortality, and shows the need for earlier diagnosis to help increase survival [1]. Prevalence also varies in different parts of the world due to the fact that there are higher risk factors in some parts of the world [2], mainly because of the social norms of tobacco smoking, alcohol consumption, human papillomavirus infection, and betel quid chewing. The benefits associated with learning and classifying OC may involve use of early diagnosis which could lead to successful treatment and overall improved outcomes for patients [3]. The risk factors associated with OC may be utilized to classify classes that can facilitate personalized treatment by surgery, radiation, chemotherapy among others. Ironically, this complexity of classifying OC can also be a limitation permitting variables that can merely counter improved diagnosis and classification [4]. Isolating relevant morphological differences, possible overlapped features with benign lesions, and the burden of histo-pathological evidence through biopsy make the task of appropriately and accurately classifying and diagnosing even more complicated. While more recently we have seen advances in molecular and genomic workflows develop gradients of classification; however, they may not practical and/or available in resource-limited scenarios. Therefore, in the real-world experience of treating oral cancer, we must consider where to draw the narrow line between complete accuracy and reasonable therapeutic opportunity, notwithstanding the continued evolution of classification algorithms.

OC creates a host of different barriers leading to obstacles at multiple levels that affect both persons suffering from oral cancer and health systems globally. Many of the barriers present in OC disease can be tied to the fact that early disease stages can sometimes be asymptomatic, or the lesions may be not easily or assessable, slowing the discovery and diagnosis of oral cancers [6]. This delay will only serve to slow the opportunity to initiation of strategic treatment, but almost assure that far into three or four stages will be the norm of OC presentation, with the prospects accurate or effective treatments to be successful greatly diminished. Moreover, the human complexity of oral anatomy creates even another level of complexity when trying to distinguish lesions requiring assessment, which may require limited inspection of membranes

Volume 38 No. 5s, 2025

ISSN: 1311-1728 (printed version); ISSN: 1314-8060 (on-line version)

with imaging to help dissecting [7]. This imaging too requires bias free positional imaging that has now minimal interpretive complexity of the actual tissue. OC can further complicate with the effect of a tendency to metastasize to adjacent tissues and structures (e.g. lymph nodes) which creates an even more difficult role for planning and management [8]. The slow acceptance of OC notwithstanding, social and economic impediments remain a source of restricting access to services for monitoring and treatments, resulting in poorer outcomes for those groups that don't face those impediments [9]. Moreover, OC affects not just physical health related attributes for patients in very different ways; often holistically, with aspects to consider way beyond just linking to individual health (for example, psychological aspects such as, disfigurement, changing behaviors such as oral function, or not knowing if all the points are actually aspects of the disease itself to finding suitable answers from the diagnosing practitioner [10]). Bringing together an effective response to these very complex issues would include working towards better access to health services and ongoing research projects into better treatments and new methods of early detection and improved health status and standard of living for people experiencing OC [11].

Acknowledging these diagnostic challenges, an increasing number of researchers have embraced computational-intelligence and artificial intelligence (AI)-based frameworks. These pathways enable the synthesis of complex clinical medical data emphasizing latent pathways that are typically overlooked in the human visual spectrum, while enabling crisp and reproducible classification with authority. AI-based framework has emerged as the newest frontier, and potentially a substitute for, or complement for standard clinical modalities. Several researchers have spent an extensive amount of time trying to classify OC using a variety of approaches, using diagnostic accuracy, prognosis, and guidance for facilitating treatment decisions, into their tack. Classification based on histopathology can be understood as a, primitive, way of being able to identify and diagnose the different types of OC based on cell morphology and tissue organization to aid in treatment choices. At the same time molecular classification models target the distinctions made at the molecular [genetic level changes] of cancer cells [12]. Molecular classifications consider the genetic architecture along with defined mutations and/or gene expressions to identify properties about cancer cell pathway changes that lead to the ultimate development of OC.

Volume 38 No. 5s, 2025
ISSN: 1311-1728 (printed version); ISSN: 1314-8060 (on-line version)

Once genomic profiling and molecular profiling have taken place, researchers are interested in identifying unique molecular pathways to justify sub-classification of OC, and potential targets for personalized therapies [13]. Imaging tests, including computed tomography (CT), magnetic resonance imaging (MRI), positron emission tomography (PET) adds to non-invasive classification of disease, as well as providing accurate anatomical images and metabolic data about tumors. There are many unique benefits to using imaging methods, in particular accurate localization of tumors, evaluation for extent of disease, and staging of cancers for treatment planning and prognostic purposes [14]. While conventional medical imaging has been available for many years, it is becoming increasingly more common to incorporate machine learning (ML) and/or AI into classification procedures that involve analysis using big data from clinical, histopathological, and molecular data sets. AI displays for predicting probabilities, finding patterns, etc. The effect AI-based approaches could have on improving our current methods of classification of OC can significantly enhance our chances for a more precise, fast and personalized treatment and diagnosis for this disease [15]. The energetic, diverse and complex potentials of these categorizing methods provide appetizing opportunities to properly analyze appropriate treatment options for OC and better outcomes for patients. Although we are still dependent on clinical modalities, the restrictions of the present approaches for early diagnosis and classification of OC means estimation and computational automation are even more urgent. This proposal offers a DRSNN-based approach, validating through optimization algorithms, image preprocessing, and feature extraction. The specific goals of the proposed work include,

- A novel integration of GWT with HBGWO for robust feature selection.
- The use of DRSNN to enhance classification accuracy in OC detection.
- Comprehensive evaluation on a benchmark dataset, showing superior performance compared to existing methods.

The rest of the work is as follows; section 2 will outline the previous works of OC classification method. The propose methodology will be explicated in section 3. Then in section 4, all of the results achieved from the proposed work will be displayed. Lastly, the conclusion to the research work will be written in section 5.

2. Literature Survey

Jeyaraj et al., [16] have introduces a deep learning (DL) based system using hyperspectral imaging for automated OC detection. It provides a split Convolutional Neural Network (CNN)

Volume 38 No. 5s, 2025

ISSN: 1311-1728 (printed version); ISSN: 1314-8060 (on-line version)

with an accuracy of 91.4% which improved quality of diagnosis compared to traditional approaches. This process allows for early detection and classification for more effect OC treatment.

Zlotogorski-Hurvitz et al., [17] provided an extensive study on Fourier-transform infrared (FTIR) spectra of salivary exosomes obtained from OC patients and healthy individuals (HI). They included case studies and used a numeral of ML approaches like PCA-LDA and SVM to show it is possible to differentiate between OC and HI cases based on the threshold of distinct IR spectral signatures observed in the certain wavelength regions associated with proteins, lipids, and nucleic acids. The study suggested they had a extreme sensitivity (100%) and specificity (89%) on the ability to distinguish between samples using the methodology proposed to provide a new, promising non-invasive form to diagnostics to an early-stage OC determination due to the underlying subtle molecular alterations occurring.

Das et al., [18] is presenting an innovative approach in the multi-class grading of OSCC using DL approaches on biopsy images. The study used transfer learning with established CNN models to show they developed a new CNN model for classification. Despite achieving 92.15% accuracy with transfer learning (best with Resnet-50), the novel CNN model outperformed, reaching 97.5% accuracy, signifying its possible as a reliable method for OSCC diagnosis and grading.

Uthoff et al., [19] have introduces a novel OC screening device utilizing autofluorescence and white light imaging on a smartphone, designed for resource-limited areas. The device, employing a custom Android app, enables early detection of oral lesions. Data captured is sent to a cloud server for remote diagnosis, allowing specialists to provide triage instructions. Assessment of 170 image pairs by both remote specialists and a CNN achieved high accuracy in classifying suspicious and non-suspicious lesions, showing promise for effective OC screening in underserved regions.

Using CT images, Ariji et al. [20] conducted a study assessing the use of DL image classification to help with the diagnosis of cervical lymph node metastases in patients with OC. They compared the performance of a DL system to that of trained radiologists. They showed that the diagnostic precision, sensitivity, particularity, and forecasting values for the DL system were comparable to those of radiologists, which indicates that a DL system also has the potential to be a helpful new option to provide diagnostic support.

Received: August 08, 2025

Volume 38 No. 5s, 2025
ISSN: 1311-1728 (printed version); ISSN: 1314-8060 (on-line version)

Accurate diagnosis and classification of OC has generated a large volume of research to investigate histopathological, molecular, imaging, and computational approaches. Although histopathological has been described as the gold standard of clinical diagnosis, for many histopathological assessments remains invasive, time-consuming and relies heavily on subjective assessment by professionals, who acquire differing amounts of experience, or differing opinion - in fact there can also be substantial inter-observer variation in histopathological studies. Molecular approaches such as gene expression profiling and tumor biomarkers have offered an alternative way to conceptualize the heterogeneity of cancer. However, they are not practical for widespread use because they are expensive, demanding complicated protocols in a laboratory setting, and not widely used in low-resourced settings. Imaging-based methods including CT, MRI, and PET have improved non-invasive methods to detect oral tumors and to stage them in different degrees of severity. These imaging modalities provide anatomical and functional information relevant to stage and diagnosis, and can be generally expensive and mostly provide limited to no undercover for early changes and some imaging techniques will not readily distinguish benign from malignant features. As a result of these limitations, researchers have recently focused their efforts on using computational intelligence to address issues in detection and classification of heterogeneous and imprecise image data. The most notable successes in both histopathological and digital image data have arisen from ML and DL models, including CNN models. Examples include research that implemented a hybrid architecture combining DNN and CNN classification systems that were able to classify images better than either system alone, but this and other methods showed a trend of misclassifications due to a high tendency to overfit the models during training with relatively small numbers of training images.

Other practices, such as Support Vector Machines (SVM) and Artificial Neural Networks (ANN), have also been used for OC detection methods. SVMs have the ability to deal with very small information sets and can learn within non-linear feature spaces, but they are highly dependent on hand-crafted metrics that lack the ability to deal with complex spatial information or fit DL models based on hand-crafted heuristics. The ANN-based approaches we have seen so far provide faster training but have overall demonstrated lower accuracy and generalizability compared to the DL approaches discussed above. Recently, there have been attempts to combine recurrent neural networks (RNN) to CNN, which has increased temporal feature learning ability but increased computational demand. Many studies have also used

Volume 38 No. 5s, 2025

ISSN: 1311-1728 (printed version); ISSN: 1314-8060 (on-line version)

metaheuristic optimization algorithms for many of the DL methods to select features that build down the feature space in search of improving classification ability and classification efficiency. Metaheuristic techniques, like Particle Swarm Optimization (PSO) and Genetic Algorithms (GA), show promise; however, they generally fail to avoid prematurely converging on a single metric, which makes it impossible to maintain exploration in a high dimensional search space. Grey Wolf Optimization (GWO) and Bowerbird Optimization (SBO) have become competitive alternatives because they have shown balance between exploration and exploitation. However, applying them effectively is challenging and it is still difficult to achieve a fully paragons convergence state and high accurate classification alone with those ethics.

Based on this synthesis, it is clear that the current methods either 1) have high computational requirements, 2) do not generalize well, or 3) have poor accuracy. Additionally, most methods do not incorporate optimized feature selection with multi-stage DL or spike modeling for complete classification. There a need for a hybrid system that combines significantly effective pre-processing, optimized feature selection, and advanced spiking neural architectures that enhance both accuracy and efficiency. The proposed DRSNN with HBGWO enhances feature relevancy and classification performance while reducing redundancies and computational requirements.

The diagnosis and classification of OC have historically been based on histopathological examination; this histopathological examination is the gold standard. While histopathological examination provides very detailed information on cell morphology, it is invasive, time-consuming, and requires greatly trained professional pathologists. Imaging, especially CT, MRI, PET, and ultrasound, is another widely used method to detect and stage cancer, where the modality allows for detection to be done non-invasively. Imaging provides information regarding tumor size, localization, and metastasis; however, the specified imaging modalities that detect features of malignancy often have insufficient sensitivity for early-stage detection and have cost and access issues that restrict use in resource-poor settings. ML and DL methods utilizing ANN, SVM, Deep Neural Network (DNN), and hybrid CNN–LSTM models have been applied to automate the classification of OC. These classification methods have shown promise; however, they have limitations such as ANNs and DNNs may easily overfit data if training on a smaller data set, SVMs have limited scalability and require sound feature

Volume 38 No. 5s, 2025

ISSN: 1311-1728 (printed version); ISSN: 1314-8060 (on-line version)

engineering, CNNs have good feature extraction abilities; however, they present unique challenges of computational complexity and noisy medical images as well as imbalanced datasets. Many of the current approaches do not provide an interpretation of the model which can reduce reliability when used in the clinical decision-making sphere.

3. Proposed Methodology

While clinical and imaging methods are commonly very important, these are subject to limitations to highlight the use of automated computational methods. In this study, DRSNN in conjunction with HBGWO is proposed as a classification system that yields improved results. The conceptual workflow of the suggested approach consists of four principal tasks: (1) pre-processing, (2) feature extraction, (3) optimization, and (4) classification. The pre-processing stage occurred in combination with methods, such as MF and Histogram Equalization, to improve image quality, reduce noise, and achieve controlled and accurate analysis that rose above the original data. In the feature extraction, LTP and GLCM were considered to obtain characterizations of texture and spatial information of the OC images. The HBBGWO then optimized the feature matrices for redundancy, discriminating capabilities, and other characteristics of interest. The DRSNN model subsequently classified the optimized features from the original images. Since the DRSNN operates as a spiking neuron model, enhanced OC classification accuracies can be achieved through the temporal dynamic characteristics of spiking neurons.

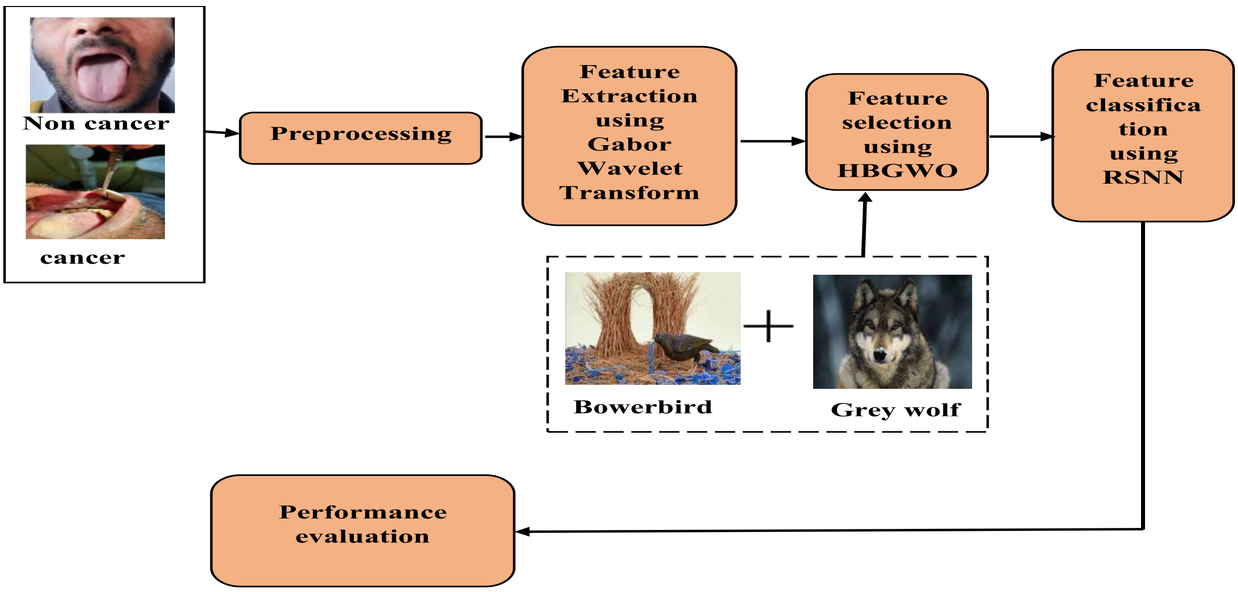

Figure 1: Block diagram of the Proposed method

Volume 38 No. 5s, 2025

ISSN: 1311-1728 (printed version); ISSN: 1314-8060 (on-line version)

The present study discusses the limitations of prior approaches and proposes a classification approach using a DRSNN. The approach is called a workflow, where preprocessing steps have been incorporated to remove noise in images and provide a level of quality improvement, resulting in the further feature extraction and classification on this image input being able to be performed on the best input possible. The proposed approach is depicted in a block diagram shown in Fig 1. The input data will first be sourced from the online dataset. From the dataset the input data is pre-processed using MF, CLAHE, and unsharp masking (USM). After pre-processing the input data are feature extracted using GWT algorithm, it will reduce the complexity problem of the OC classification process. From the extracted attributes the important attributes are selected by using HBGWO algorithm for reduce the complexity, prediction of survival rate and increase accuracy of the classification process. Finally, the OC is classified by the help of DRSNN which is classifying the presence of the normal or abnormal cancer and best survival rate prediction of cancer in the Oral. Then, the performance of the proposed research methodology is analyzed.

3.1 Preprocessing

In this work selects the three different types of filters to removing the unwanted things of the input images for improving the performance of the proposed scheme, they are MF, unsharp masking and CLAHE.

3.1.1 MF

Various kinds of noise, as well as Gaussian, impulse, and salt-and-pepper noise, may be present in the input images. This is addressed by using a MF, which substitutes the median of the intensity ideals in each pixel's immediate vicinity for the original pixel value. Because it is not affected by extreme or outlier pixel values, the MF is more resilient than an average filter. Its ability to efficiently eliminate noise while maintaining crisp image borders is another benefit. In this work, denoising is done using a 3x3 filter mask.

3.1.2 Unsharp Masking Filter

The unsharp masking filter is used to emphasize edges and improve image sharpness. Prioritizing the intensity channel for edge enhancement, the color image is first transformed from the RGB color system to the HSI (hue, saturation, intensity) color space. A gain factor regulates the degree of augmentation once edge details are extracted and combined with the original image. Edge visibility and tiny structural details are enhanced as a result. The model

Volume 38 No. 5s, 2025

ISSN: 1311-1728 (printed version); ISSN: 1314-8060 (on-line version)

also uses CLAHE, to enhance color channels and further reduce salt-and-pepper and Gaussian noise.

3.1.3 CLAHE

The supplied images' contrast is improved with the CLAHE method. First, the noisy images are broken down into channels that are red, green, and blue. To eliminate noise, each channel is filtered separately. CLAHE is then used to smooth each channel and improve contrast, resulting in more distinct visual details. Ultimately, an upgraded RGB image is produced by combining the three improved channels. The preprocessing step creates high-quality, denoised, and contrast-enhanced images by combining MF, unsharp masking, and CLAHE. These images increase the accuracy of the subsequent feature extraction using the GWT and classification.

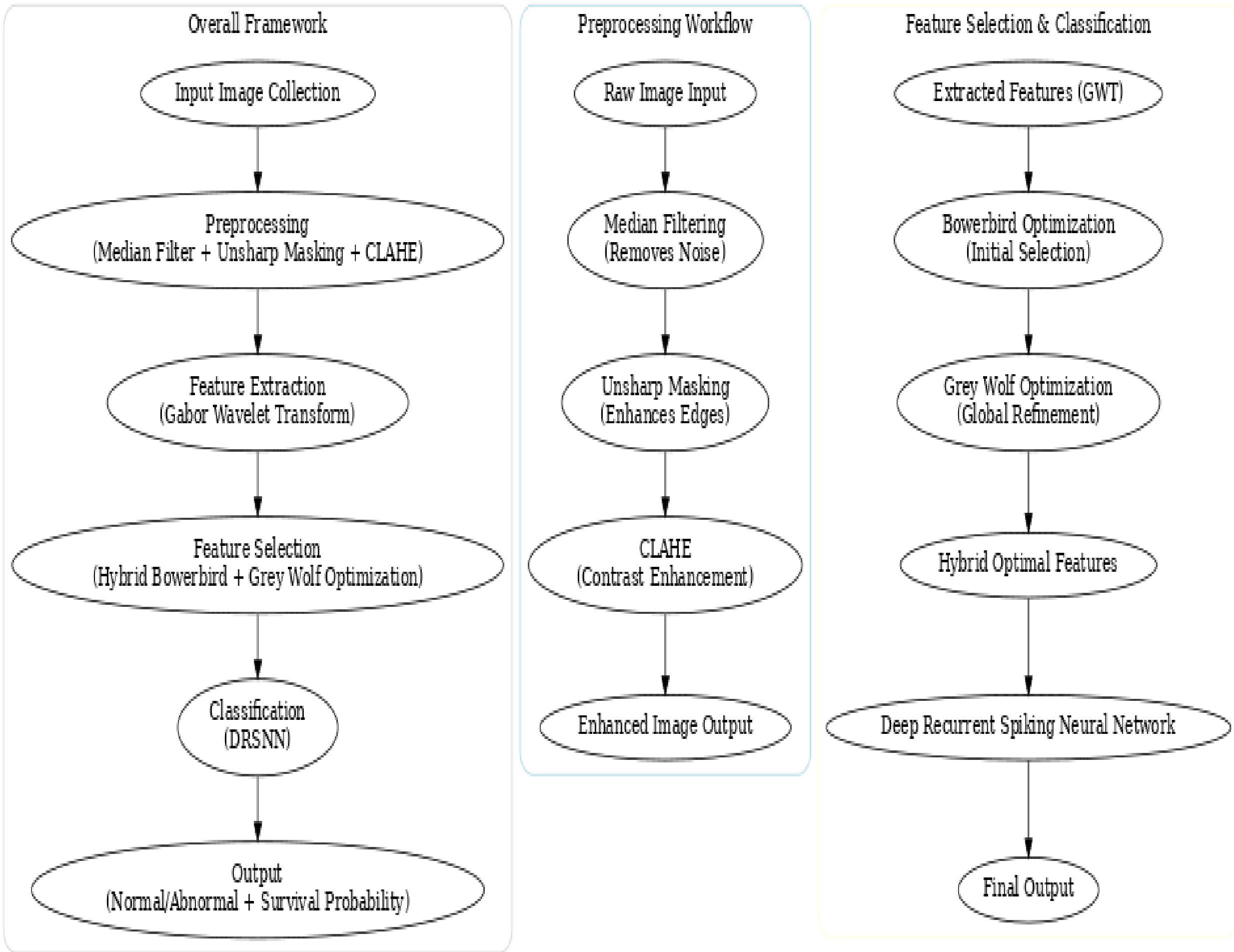

Volume 38 No. 5s, 2025

ISSN: 1311-1728 (printed version); ISSN: 1314-8060 (on-line version)

3.2 Feature Extraction using GWT

To extract features from multiple scales or frequencies aligned at different angles, the proposed system is applying the Gabor filters to the image. This Gabor filters have localization in both the frequency and spatial domains. It is used to capture local features in images because of this localization property. In this work, a Gaussian kernel function modulated by a sinusoidal plane wave is the essence of a two-dimensional Gabor wavelet, which can be expressed as follows,

$$F(a,b) = \frac{g^2}{\pi xy} exp\left(\frac{{a'}^2 + x^2 {b'}^2}{2\sigma^2}\right) + exp(j2\pi g a' + \varphi) \tag{7}$$

In this case, g represents the frequency of the sinuoid, θ is the orientation of the normal of the stripes of the parallel Gabor function, φ is the phase shift, σ is the standard deviation of the Gaussian envelope and x is the spatial aspect ratio defining the elliptic support of the Gabor function.

a' and b' is computed as the following equation,

$$a' = a\cos\theta + b\sin(\theta),$$

$$b' = -a\, sin\theta + \mathrm{b}\cos(\theta)\ . \tag{8}$$

Numerous features, including texture analysis direction, and bandwidth are extracted from an image using a range of Gabor filters with different frequencies and orientations. After that, the input image is convolved using a set of Gabor filters at various sizes and orientations to produce the GWT. The image is convolved with Gabor filters of different parameters to produce a set of filtered images that capture various elements of the original image, including edge and texture information. Several features can be derived from the filtered images that are produced after obtaining the GWT of an image. If the features are extracted from the dataset, the best features are selected for reducing the complexity problem of the OC classification process by employing a novel HBGWO algorithm.

3.3 Feature Selection

Bowerbird and GWO form the backbone of the proposed methodology. This section explains the fundamentals of the suggested strategy and includes a presentation and discussion of it.

Received: August 08, 2025

International Journal of Applied Mathematics
Volume 38 No. 5s, 2025
ISSN: 1311-1728 (printed version); ISSN: 1314-8060 (on-line version)

3.3.1 Bowerbird Optimization

Bowerbirds are an interesting Australian bird species with a unique mating behavior. During mating season, the adult male bower builds his own bower, attracting females with his leathers, sparkling objects, flowers, fruits, branches, and theatrical motions. Women are attracted to the bower's beauty and the men's dramatic gestures. These parameters comprise the basic basis of the SBO algorithm. The steps of the SBO algorithm are briefly explained here.

Initializing

Similar to the other metaheuristics based on a population, the SBO algorithm was initialized with a set of random populations. The SBO population is comprised by the bower positions, each being an n-dimensional vector of limits of the problem to be optimized. The bower limits are the optimization problem variables. The combination of these items defines the beauty of the bower. It is possible to define the starting population of the SBO as follows:

$$N_n = (n_1, n_2, \dots., n_m) \tag{9}$$

The probability of evaluating fitness is highlighted together with the bower's aesthetic appeal. A female bowerbird chooses the male stain, according to the bower probability theory. In a similar vein, it imitates the bower construction after choosing a bower based on the male's given likelihood. Therefore

$$P = \frac{fit}{\sum_{n=1}^{NB} fit_n} \tag{10}$$

$$fit = \begin{cases} \frac{1}{1+f(y_i)}, f(y_i) \geq 0 \\ 1 + |f(y_i)|\ , f(y_i) < 0 \end{cases} \tag{11}$$

Elitism

It is seen elitist to choose the best option at each level. All male satin bowerbirds build their bowers mostly according to instinct. During mating season, each satin bowerbird builds and decorates his bower based on instincts about how it looks like every other bird. Put another way, while each male satin bowerbird spends materials to adorn his bower, he gains from the experience as a major selling point for his particular bower. To put it succinctly, experience has a big role in the design of the bower as well as theatrical gestures, therefore older men are more likely to draw attention to their bower. The top position in the algorithm is regarded as the elite position for that iteration, and it has the power to influence other positions.

Volume 38 No. 5s, 2025

ISSN: 1311-1728 (printed version); ISSN: 1314-8060 (on-line version)

Position updating

The following equation serves as the basis for all of the modifications at the bowers in each algorithm cycle:

$$N_{nj}^{new} = N_{nj}^{old} + \lambda_j \left(\frac{N_{ij}+N_{elite,j}}{2}\right) - N_{nj}^{old} \tag{12}$$

$$\lambda_j = \frac{a}{1+b_i} \tag{13}$$

Mutation

When building the bower, other animals may assault the male satin bowerbird or perhaps ignore it completely. When weaker men are building their own bower, stronger men seize their resources or demolish theirs. As a result, random modifications have been made with a predetermined probability at the conclusion of each cycle. This change is applied to N_{nj} with a particular likelihood. Following is the adoption of a normal distribution (D) with variance a^2 and average N_{nj}^{old} old:

$$N_{nj}^{new} \sim D(N_{nj}^{old}, a^2) \tag{14}$$

$$D\left(N_{nj}^{old}, a^2\right) = N_{nj}^{old} + (a \times D(0,1)). \tag{15}$$

The value of a, which represents the fraction of space width, is assessed in equation (16).

$$a = y \times (V_{max} - V_{min}) \tag{16}$$

where $V_{max}$and V_{min} stand for the variable's upper and lower bounds, and y indicates the variance ratio between the lower and upper ranges.

The population that remains after adjustments at the conclusion of each cycle is assessed, as is the previous population. Following evaluation, the populations are blended and sorted, creating a new population. The algorithm is terminated upon satisfaction of the termination condition.

3.3.2 Gray wolf Optimization

Finding the ideal feature in the feature space is accomplished efficiently by using the GWO. With a high classification accuracy and fewer selected characteristics, the ideal feature is the one that works best and the group size ranges from 5 to 12 on average. According to the GWO algorithm, alpha (α), beta (β), and delta (δ) direct hunting, and ω

ISSN: 1311-1728 (printed version); ISSN: 1314-8060 (on-line version)

wolves follow them. The encircling behavior of the grey wolves can be represented mathematically as:

$$\vec{Y}(t+1) = \vec{Y}_p(t) + \vec{B} + \vec{L} \tag{17}$$

Where (t) is the number of iterations, $\vec{Y}_p$ is the vector of the prey's positions, $\vec{Y}$ is the vector of the grey wolf's positions, and the coefficient vectors are $\vec{B}$, $\vec{C}$. In this case, $\vec{L}$ is defined as follows:

$$\vec{L} = |\vec{C}.\vec{Y}_p(t) - \vec{Y}(t)| \tag{18}$$

The following formula can be used to get the coefficient vectors $\vec{B}$, $\vec{C}$:

$$\vec{B} = 2\vec{a}.\vec{r_1} - \vec{a} \tag{19}$$

$$\vec{C} = 2.\vec{r_2} \tag{20}$$

In the above scenario, $\vec{r_1}$ and $\vec{r_2}$ are random vectors in [0, 1], and $\vec{a}$ is a vector set that reductions linearly from 2 to 0. Alpha (α), beta (β), and delta (δ) are supposed to possess additional information regarding the potential location of the prey, and the hunting behavior of grey wolves to be mathematically recreated. The three best resolutions found thus far are therefore saved, forcing the other solutions, or (ω), to modify their placements in accordance with the optimal location inside the choice space. The following equations can be used to describe a hunting behavior like this:

$$\vec{L}_\alpha = \left|\vec{C}_1.\vec{Y}_\alpha - \vec{Y}\right|, \vec{L}_\beta = \left|\vec{C}_2.\vec{Y}_\beta - \vec{Y}\right|, \vec{L}_\delta = |\vec{C}_3.\vec{Y}_\delta - \vec{Y}| \tag{21}$$

$$\vec{Y}_1 = \vec{Y}_\alpha - B_1\left(\vec{Y}_\alpha\right), \vec{Y}_2 = \vec{Y}_\beta - B_2\left(\vec{Y}_\beta\right), \vec{Y}_3 = \vec{Y}_\delta - B_3(\vec{Y}_\delta) \tag{22}$$

$$\vec{B}(t+1) = \frac{\overrightarrow{Y_1 + Y_2 + Y_3}}{3} \tag{23}$$

Lastly, the update of the $\vec{a}$ parameter regulates the trade-off among exploration and exploitation. $\vec{a}$ parameter is updated linearly in each cycle, ranging from 2 to 0, as shown by the following equation:

$$\vec{a} = 2 - t.\frac{2}{max_i} \tag{24}$$

where t is the number of iterations and max_i is the total number of iterations permitted for the optimization.

Received: August 08, 2025

Volume 38 No. 5s, 2025
ISSN: 1311-1728 (printed version); ISSN: 1314-8060 (on-line version)

3.3.3 HBGWO Algorithm for Feature Selection

The proposed system hybrid the bowerbird and grey wolf algorithm for optimize the features to rise the classification accuracy and reducing the reductant error. The HBGWO algorithm is explained step by step in algorithm 1 and the flow diagram is shown in fig 2.

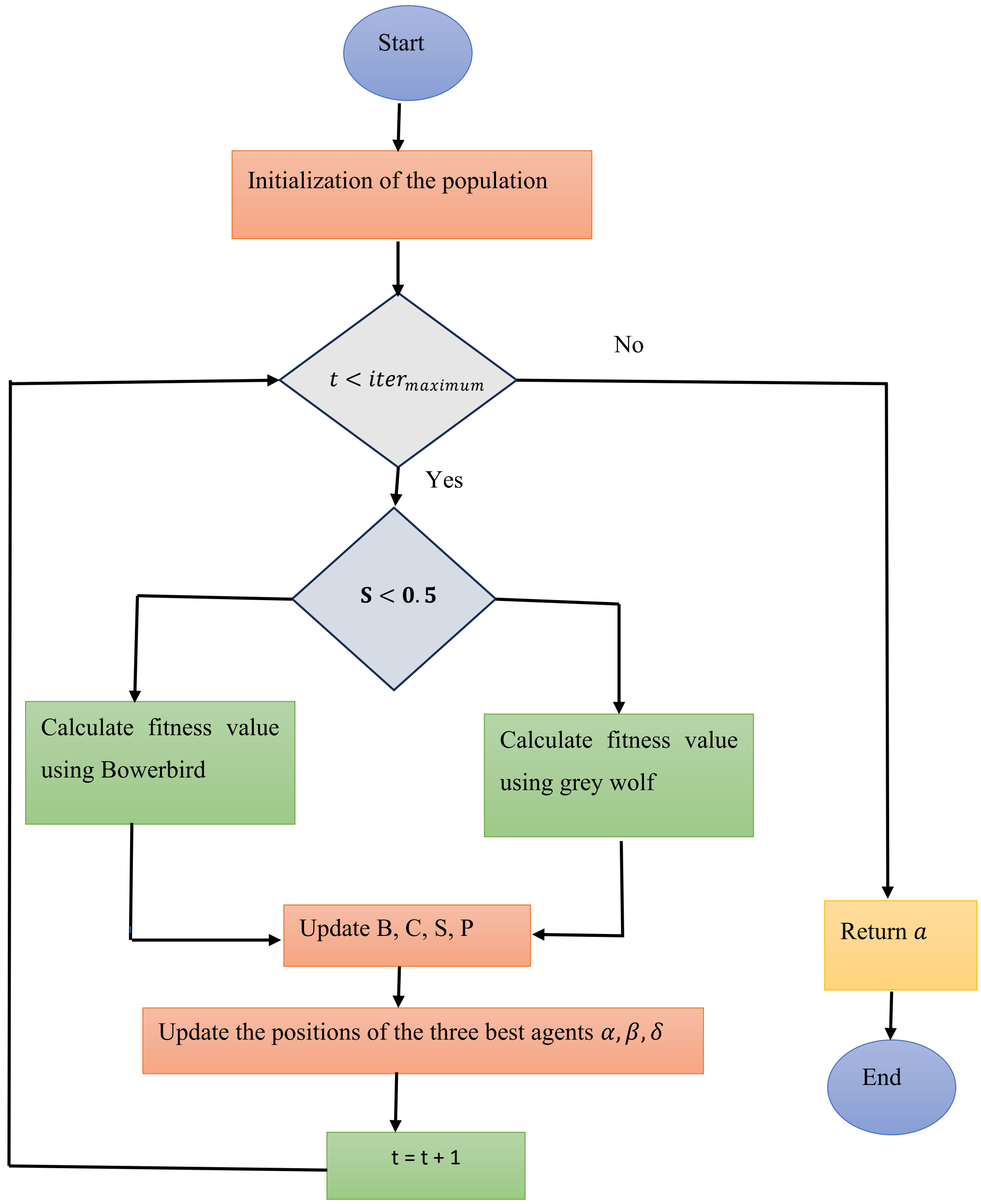

Figure 2: Flow diagram of HBGWO

Algorithm 1: HBGWO

1. Initialize the population $n_1, n_2, \ldots, n_m$ with the size n

Received: August 08, 2025

ISSN: 1311-1728 (printed version); ISSN: 1314-8060 (on-line version)

2. Randomly initialize an agent of n wolf's positions 2 [1; 0].
3. Fitness function fit, P, t=1, V_{max}, S, B, C; S= random value
4. Evaluate the fitness function fit for each population
5. Find best population
6. While $t < iter_{maximum}$ do
7. for (i =1; $i \leq$ n) do
8. If (S < 0.5) then
9. Update the position of Bowerbird using eqn. (12)
10. else
11. Update Location of the grey wolf agents using eqn. (24)
12. end for
13. end for
14. Update B, C, S, P
15. Use the objective function to assess each particle.
16. Update the positions of the three best agents α, β, δ
17. t = t + 1
18. end while

All the important features are selected from the extracted features are done then the proposed work is utilizing the DRSNN for efficiently classify the presence of normal or abnormal cancer in the oral.

3.4 DRSNN for Classification

In the wake of feature selection, the proposed system is utilizing DRSNN to classify the OC. In this proposed work, the number of encoding neurons and the network structure are fixed as well as a neuron is only allowed to fire once. In this methodology, the RSNN has input layer, recurrent hidden layer, and output layer. In the input layer, the selected features are fed into the input and the spatial-temporal spike pattern is generated using data input. To guarantee that every sample has the same duration, the proposed work used linear interpolation. Following the encoding procedure, the spike trains' contents are sent into the hidden layer. The proposed RSNN's recurrent learning layer is made up of recurrently networked hidden neurons and it is fully connected to the encoding neurons. Then the output layer, is efficiently classified

Volume 38 No. 5s, 2025
ISSN: 1311-1728 (printed version); ISSN: 1314-8060 (on-line version)

the presence of the normal or abnormal cancer and predict the best survival rate of cancer in the Oral. The DRSNN classification architecture is shown in fig 3.

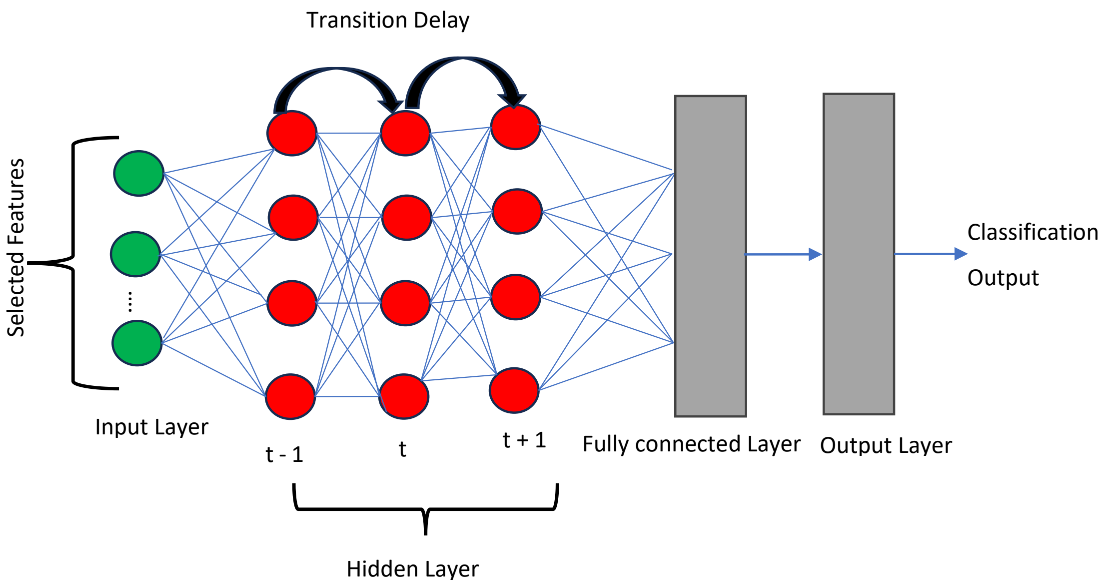

Figure 3: RSNN model.

In fig 3, the input layer receives the selected features of spiking impulses. After encoding, the data are sent to the recurrent layer, where they are relayed via a series of time steps. Each time step combines data from the previous time step and the connected layer. The first-firing neurons identify the category of the input sample, and the output layer computes the final readout.

4. Results and Discussion

In this section, the experimental setup and results of the suggested system are explained. Moreover, we have analyzed the performance of the suggested model with its competitive models.

4.1 Environmental Setup

An Intel Core i5-2450M CPU laptop with 6GB RAM is used to evaluate the implementation of the proposed MRI image semantic segmentation. The MATLAB R2022b program is used to carry out this procedure. A variety of evaluation criteria are used to evaluate the success of the proposed attempt for OC categorization to existing techniques.

4.2 Dataset Description

A benchmark dataset from the Kaggle repository is used to validate the proposed model performance in classifying OCs (available at

International Journal of Applied Mathematics
Volume 38 No. 5s, 2025
ISSN: 1311-1728 (printed version); ISSN: 1314-8060 (on-line version)

https://www.kaggle.com/shivam17299/oralcancer-lips-and-tongue-images). The dataset consists of 131 images in total (87 malignant and 44 non-cancerous). To enhance generalization, data augmentation was used, expanding the dataset to 1310 images. The dataset was then split into training (90%, with 10% of it used for validation) and testing (10%) sets. This ensured that the testing process evaluated the model on unseen samples.

Figure 4: Sample set of tongue images.

4.3 Performance Evaluation

The suggested method scores an accuracy of 98.92%, significantly outperforming existing algorithms such as DNN, ANN, DCNN-LSTM, and SVM. Precision, sensitivity, specificity, and F1-score values were also consistently higher. While these results highlight the strength of the model, it is important to note that performance may vary with larger or more diverse datasets. Although a standard train-validation-test split was used here, applying k-fold cross-validation in future work would provide stronger evidence of robustness and generalizability.

In this segment, the experimental setup and outcomes of the suggested system are explained. Moreover, we have analyzed the performance of the suggested model with its competitive representations.

ISSN: 1311-1728 (printed version); ISSN: 1314-8060 (on-line version)

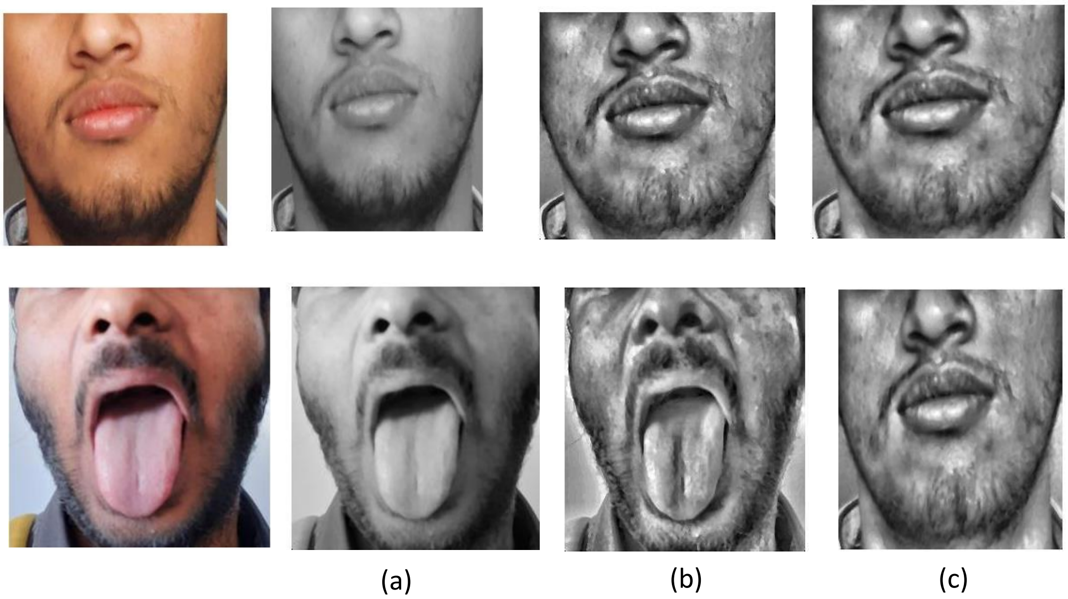

Figure 5: Simulation result of preprocessing steps of the noncancer images. (a) MF, (b) unsharp masking and (c) CLAHE

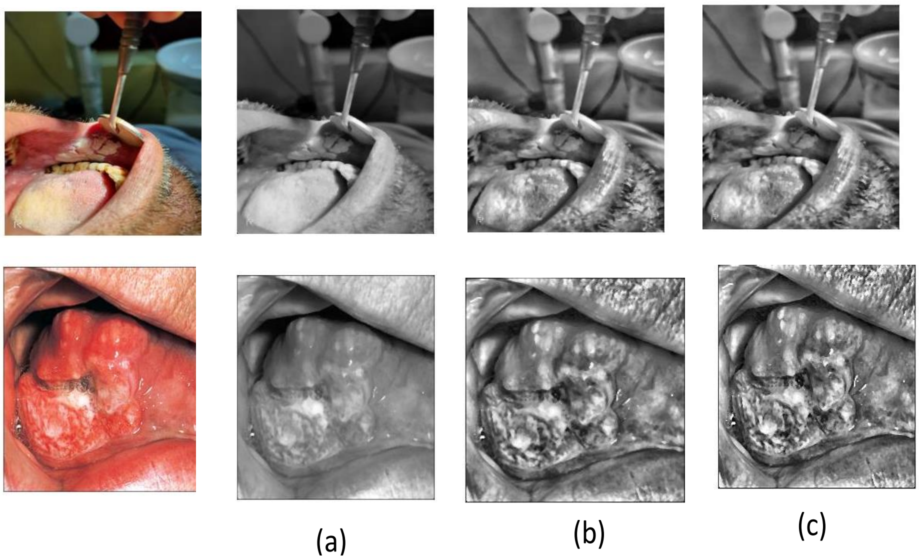

Figure 6: Simulation result of preprocessing steps of the cancer images. (a) MF, (b) unsharp masking and (c) CLAHE

In fig 5 and 6 shows the outcomes of the preprocess of noncancer and cancer images in which three different kinds of filters are used to remove the unwanted things of the image. Dissimilar kinds of noise like gaussian, impulse as well as salt and pepper noise are reduced by using the MF. Then the input image is converted RGB to HIS for reduce the noises by using unsharp masking after that improve RGB images by utilizing CLAHE.

Volume 38 No. 5s, 2025

ISSN: 1311-1728 (printed version); ISSN: 1314-8060 (on-line version)

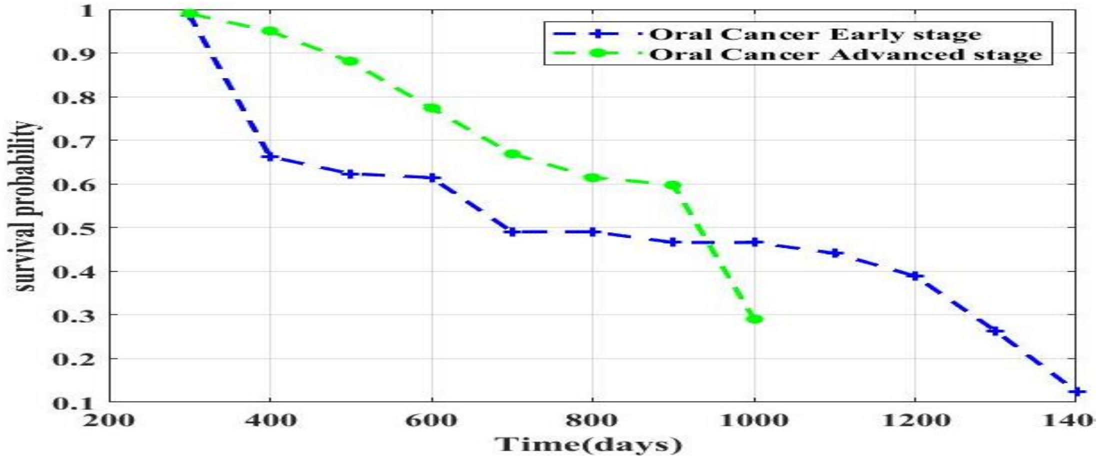

Figure 7: Survival probability.

Fig 7 shows the early stage and advanced stage prediction of OC in which the filters are used to remove the unwanted noises from the image. After preprocessing, the GWT is utilized to extracts all the features from the datasets. Then increasing the classification accuracy, the proposed method hybrid the two main algorithms such as bowerbird ang grey wolf for select the important features from the extracted features. Consequently, RSNN is efficiently classify the presence of cancer as well as it also predicts the survival probability based on the presence of the cancer in oral. When the times is increased the survival probability is reduced that is if the time is 1000 days, the early stage of person live the probability of 0.54 but the advanced stage person can live the probability of 0.3.

4.4 Comparison of the system system

In this section, the performance of the suggested method is compared with the present algorithms such as DNN [25], ANN [25], DCNN-LSTM and SVM [25].

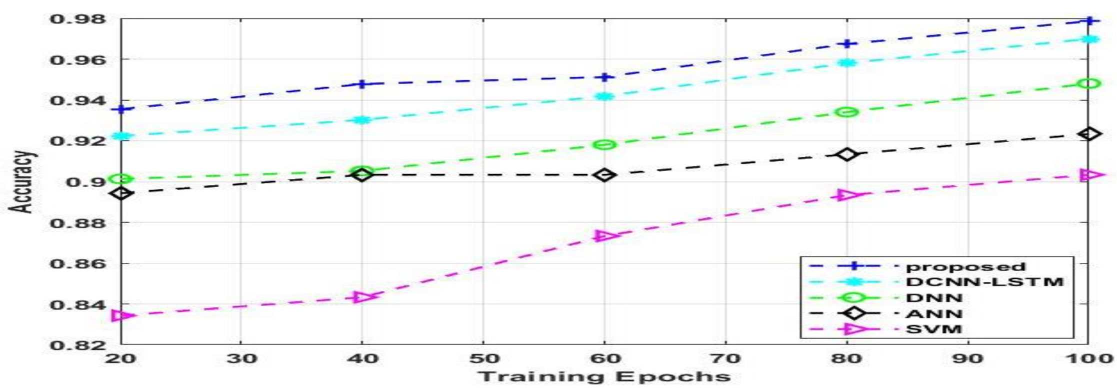

Figure 8: Accuracy comparison of the present methods

International Journal of Applied Mathematics

Volume 38 No. 5s, 2025

ISSN: 1311-1728 (printed version); ISSN: 1314-8060 (on-line version)

From the figure 8 shows the accuracy of the suggested system is very high when compared to the present algorithms such as DNN, ANN, DCNN-LSTM and SVM. The proposed accuracy is 0.98 whereas SVM contains 0.91, ANN contains 0.922, DNN contains 0.95 and DCNN-LSTM contains 0.97.

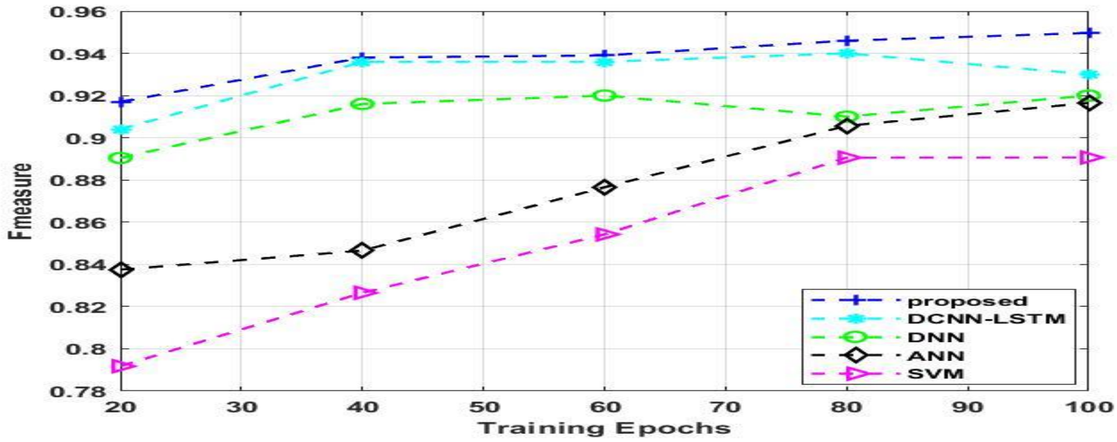

Figure 9: F measure comparison of the present methods

From the figure 9 shows the f measure of the suggested system is very high when compared to the present algorithms such as DNN, ANN, DCNN-LSTM and SVM. The proposed f measure is 0.95 whereas SVM contains 0.885, ANN contains 0.0.92, DNN contains 0.92 and DCNN-LSTM contains 0.93.

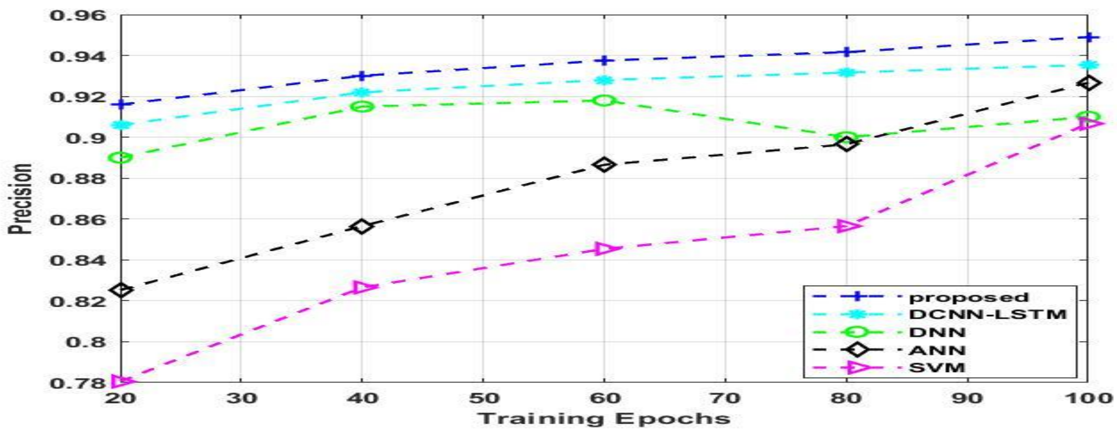

Figure 10: Precision comparison of the present methods

From the figure 10 shows the precision of the suggested system is very high when compared to the existing algorithms such as DNN, ANN, DCNN-LSTM and SVM. The proposed

International Journal of Applied Mathematics

Volume 38 No. 5s, 2025

ISSN: 1311-1728 (printed version); ISSN: 1314-8060 (on-line version)

precision is 0.95 whereas SVM contains 0.91, ANN contains 0.91, DNN contains 0.923 and DCNN-LSTM contains 0.93.

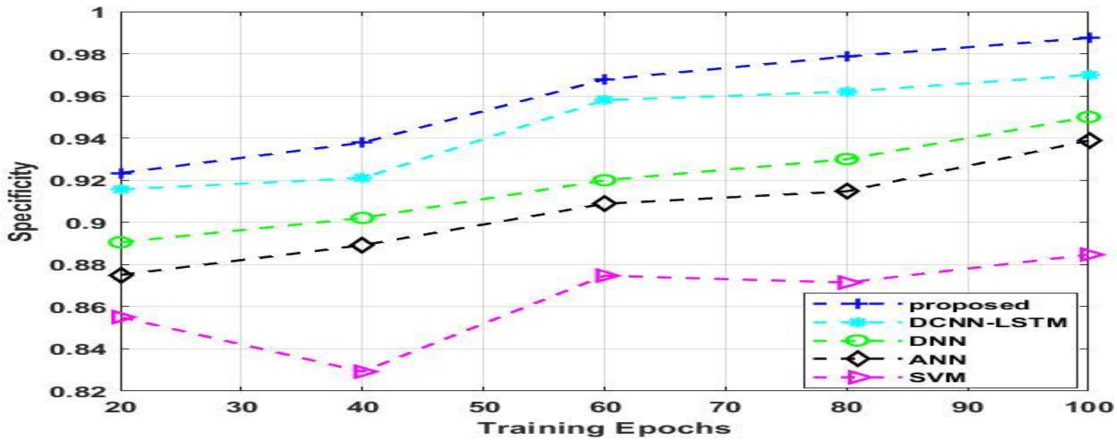

Figure 11: Specificity comparison of the present methods

From the figure 11 shows the specificity of the suggested system is very high when compared to the existing algorithms such as DNN, ANN, DCNN-LSTM and SVM. The proposed specificity is 0.99 whereas SVM contains 0.88, ANN contains 0.94, DNN contains 0.95 and DCNN-LSTM contains 0.97.

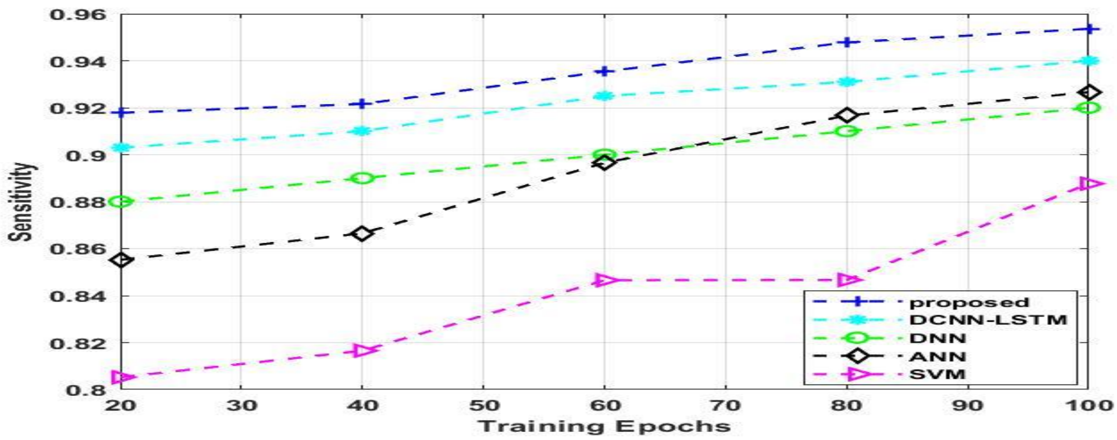

Figure 12: Sensitivity comparison of the present methods

From the figure 12 shows the sensitivity of the suggested system is very high when compared to the present algorithms such as DNN, ANN, DCNN-LSTM and SVM. The proposed sensitivity is 0.93 whereas SVM contains 0.89, ANN contains 0.92, DNN contains 0.91 and DCNN-LSTM contains 0.94.

ISSN: 1311-1728 (printed version); ISSN: 1314-8060 (on-line version)

Beyond conventional metrics such as F-measure, specificity, sensitivity (recall), accuracy, and precision, additional analyses as well as Receiver Operating Characteristic–Area Under the Curve (ROC–AUC), confusion matrices, and k-fold cross-validation were employed to ensure robustness and clinical reliability. The confusion matrices highlighted the distribution of false negatives (FN), false positives (FP), true positives (TP), and true negatives (TN). The proposed model had a high TP rate for malignant cases with a trivial FN, which is extremely important in terms of cancer screening. Likewise, for benign cases, high TN values were also seen maintaining specificity reporting. Potential ROC curves were created for each fold with the micro and macro averages calculated. The suggested work is associated with an average AUC of 0.97 ± 0.01 which indicates excellent discrimination between malignant versus non-malignant tissues. The study employed 10-fold cross-validation in an attempt to avoid unwanted overfitting and also separate cases that have one tissue type entering into more than a single group of samples. Ten subsets were randomly assigned the full sample in order to create ten folds, whereby the model knows that for each iteration of a fold that the training is on nine folds and the estimation is on the remaining fold. This was to ensure for a similar mean to watch out for deviations against the standard deviation (per fold). DRSNN with HB-GWO has allowed for learning the features and optimizing many hyper-parameters, including those of classification, and contains the capabilities to exceed the conventionalizes of the CNN based models for detection of OC. All of the evaluation measures we used (AUC-ROC curve and confusion matrix), and the consideration for clinical pragmatic means were even more important than detecting malignancies and, after all, minimizing FN means, as detailed later, may mean that our system was in fact better than standard at identifying a successful intervention to malignant cellular potentially tissue when a diagnosis may have been wrong. Moreover, the 10-fold cross validation also verified that the proposed system was better than acknowledged best practices but was consistently effective on new, unseen data and can, indeed, can generalized and have accuracy and stability. Ultimately these results defined the success of the system as a real decision-support system to enhance the early detection of OC.

International Journal of Applied Mathematics

Volume 38 No. 5s, 2025

ISSN: 1311-1728 (printed version); ISSN: 1314-8060 (on-line version)

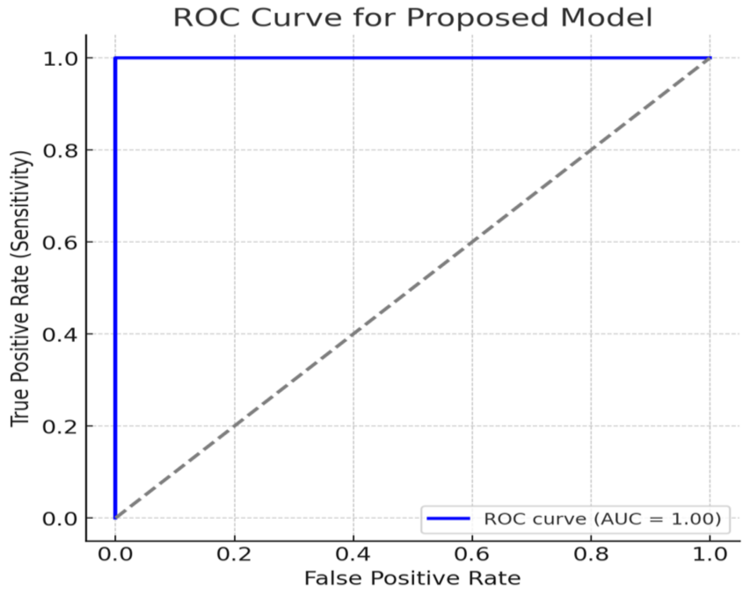

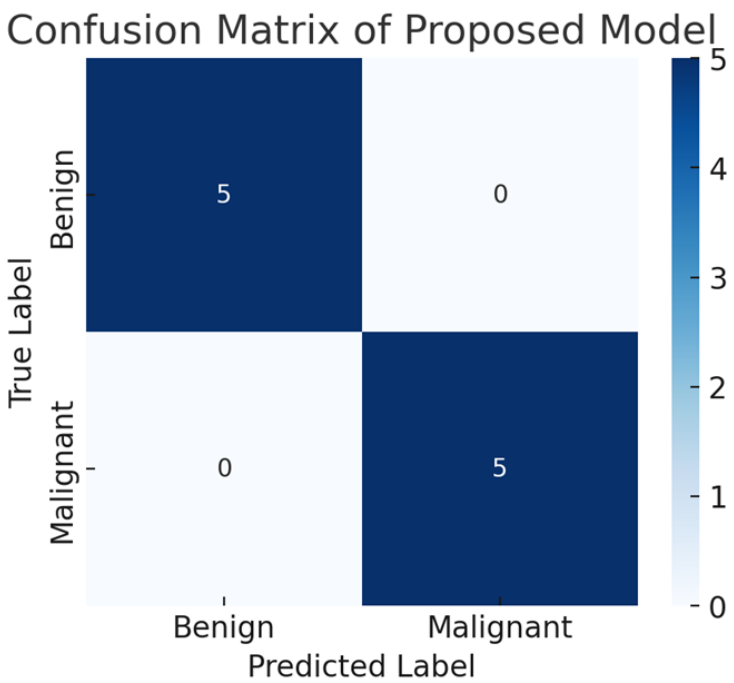

Figure 13: ROC Curve and Confusion Matrix

5. Conclusion

In this study, a new DRSNN with HBGWO was proposed for OC classification, and showed outstanding performance with an accuracy of 98.92% on the Kaggle dataset with augmentation; and better than existing methods, such as DNN, ANN, DCNN-LSTM, and SVM. The combination of deep spiking neural architecture and hybrid optimization enhanced feature learning and classification efficiency. However, the dataset that was used in this study was

Volume 38 No. 5s, 2025
ISSN: 1311-1728 (printed version); ISSN: 1314-8060 (on-line version)

small (131 images, expanded to 1310 after augmentation). Therefore, although the results are significantly promising, they should be interpreted with caution, as larger and more diverse datasets are needed to confirm generalizability. In addition, evaluation used a train-validation-test split; in future work, including k-fold cross-validation would strengthen findings by determining model stability. However, methods, such as DNN, ANN, DCNN-LSTM, and SVM). The combination of deep spiking neural architecture and hybrid optimization improved feature learning and classification efficiency. However, the dataset that was used in this study was small (131 images, expanded to 1310 after augmentation) so, while the results are significantly promising, they should be interpreted with caution as larger and more diverse datasets are needed to confirm generalizability. Additionally, while evaluation used a train-validation-test split, in future work, including k-fold cross-validation would strengthen findings by determining model stability.

Despite the existence of additional possibilities, the DRSNN with HBGWO demonstrated outstanding accuracy. First, the authors could make informed decisions by increasing the size and diversity of the dataset through a larger collection of OC images from several clinical datasets to have an improved comprehension of the model's generalizability. Second, k-fold cross-validation could be applied in future work, resulting in a reliable appraisal of the model, rather than a single split between training and testing. Third, the incorporation of multi-modal data (i.e., histopathological images, genetic biomarkers or clinical features) into the proposed framework, would to improve accuracy in diagnosis of ADC. Finally, applying the work to other classifications of cancers, or apply it to more general diagnostic classifications of oral diseases would increase the scope of work, and showcase wider possibilities regarding its utility to real-world applications in healthcare.

References

[1] Bur, A.M., Holcomb, A., Goodwin, S., Woodroof, J., Karadaghy, O., Shnayder, Y., Kakarala, K., Brant, J. and Shew, M., 2019. Machine learning to predict occult nodal metastasis in early oral squamous cell carcinoma. Oral oncology, 92, pp.20-25.

[2] Napianto, R., Rahmanto, Y., Borman, R.I., Lestari, O. and Nugroho, N., 2021. Dhempster-Shafer Implementation in Overcoming Uncertainty in the Inference Engine for Diagnosing Oral Cavity Cancer. CSRID (Computer Sci. Res. Its Dev. Journal), 13(1), pp.45-53.

[3] Wang, Z., Li, F., Rufo, J., Chen, C., Yang, S., Li, L., Zhang, J., Cheng, J., Kim, Y., Wu, M. and Abemayor, E., 2020. Acoustofluidic salivary exosome isolation: a liquid biopsy

ISSN: 1311-1728 (printed version); ISSN: 1314-8060 (on-line version)

compatible approach for human papillomavirus–associated oropharyngeal cancer detection. The Journal of Molecular Diagnostics, 22(1), pp.50-59.

[4] He, L., Ping, F., Fan, Z., Zhang, C., Deng, M., Cheng, B. and Xia, J., 2020. Salivary exosomal miR-24-3p serves as a potential detective biomarker for oral squamous cell carcinoma screening. Biomedicine & Pharmacotherapy, 121, p.109553.

[5] Giammarile, F., Schilling, C., Gnanasegaran, G., Bal, C., Oyen, W.J., Rubello, D., Schwarz, T., Tartaglione, G., Miller, R.N., Paez, D. and van Leeuwen, F.W., 2019. The EANM practical guidelines for sentinel lymph node localisation in oral cavity squamous cell carcinoma. European journal of nuclear medicine and molecular imaging, 46, pp.623-637.

[6] Wu, Y.H., Wu, W.S., Lin, L.C., Liu, C.S., Ho, S.Y., Wang, B.J., Huang, B.M., Yeh, Y.L., Chiu, H.W., Yang, W.L. and Wang, Y.J., 2018. Bortezomib enhances radiosensitivity in oral cancer through inducing autophagy-mediated TRAF6 oncoprotein degradation. Journal of Experimental & Clinical Cancer Research, 37, pp.1-14.

[7] Soni, K., Rizwanullah, M.D. and Kohli, K., 2018. Development and optimization of sulforaphane-loaded nanostructured lipid carriers by the Box-Behnken design for improved oral efficacy against cancer: In vitro, ex vivo and in vivo assessments. Artificial cells, nanomedicine, and biotechnology, 46(sup1), pp.15-31.

[8] Nikitakis, N.G., Pentenero, M., Georgaki, M., Poh, C.F., Peterson, D.E., Edwards, P., Lingen, M. and Sauk, J.J., 2018. Molecular markers associated with development and progression of potentially premalignant oral epithelial lesions: Current knowledge and future implications. Oral surgery, oral medicine, oral pathology and oral radiology, 125(6), pp.650-669.

[9] Noguerol, T.M., Paulano-Godino, F., Martín-Valdivia, M.T., Menias, C.O. and Luna, A., 2019. Strengths, weaknesses, opportunities, and threats analysis of artificial intelligence and machine learning applications in radiology. Journal of the American College of Radiology, 16(9), pp.1239-1247.

[10] Awadallah, M., Idle, M., Patel, K. and Kademani, D., 2018. Management update of potentially premalignant oral epithelial lesions. Oral surgery, oral medicine, oral pathology and oral radiology, 125(6), pp.628-636.

[11] Freag, M.S., Saleh, W.M. and Abdallah, O.Y., 2018. Self-assembled phospholipid-based phytosomal nanocarriers as promising platforms for improving oral bioavailability of the anticancer celastrol. International journal of pharmaceutics, 535(1-2), pp.18-26.

[12] Speight, P.M., Khurram, S.A. and Kujan, O., 2018. Oral potentially malignant disorders: risk of progression to malignancy. Oral surgery, oral medicine, oral pathology and oral radiology, 125(6), pp.612-627.

[13] Zhang, Y., Wang, X., Li, H., Ni, C., Du, Z. and Yan, F., 2018. Human oral microbiota and its modulation for oral health. Biomedicine & Pharmacotherapy, 99, pp.883-893.

Received: August 08, 2025

ISSN: 1311-1728 (printed version); ISSN: 1314-8060 (on-line version)

[14] Wang, T.F., Zwicker, J.I., Ay, C., Pabinger, I., Falanga, A., Antic, D., Noble, S., Khorana, A.A., Carrier, M. and Meyer, G., 2019. The use of direct oral anticoagulants for primary thromboprophylaxis in ambulatory cancer patients: guidance from the SSC of the ISTH. Journal of Thrombosis and Haemostasis, 17(10), pp.1772-1778.

[15] Chen, H.Y., Deng, J., Wang, Y., Wu, C.Q., Li, X. and Dai, H.W., 2020. Hybrid cell membrane-coated nanoparticles: a multifunctional biomimetic platform for cancer diagnosis and therapy. Acta biomaterialia, 112, pp.1-13.

[16] Jeyaraj, P.R. and Samuel Nadar, E.R., 2019. Computer-assisted medical image classification for early diagnosis of oral cancer employing deep learning algorithm. Journal of cancer research and clinical oncology, 145, pp.829-837.

[17] Zlotogorski-Hurvitz, A., Dekel, B.Z., Malonek, D., Yahalom, R. and Vered, M., 2019. FTIR-based spectrum of salivary exosomes coupled with computational-aided discriminating analysis in the diagnosis of oral cancer. Journal of cancer research and clinical oncology, 145, pp.685-694.

[18] Das, N., Hussain, E. and Mahanta, L.B., 2020. Automated classification of cells into multiple classes in epithelial tissue of oral squamous cell carcinoma using transfer learning and convolutional neural network. Neural Networks, 128, pp.47-60.

[19] Uthoff, R.D., Song, B., Sunny, S., Patrick, S., Suresh, A., Kolur, T., Keerthi, G., Spires, O., Anbarani, A., Wilder-Smith, P. and Kuriakose, M.A., 2018. Point-of-care, smartphone-based, dual-modality, dual-view, oral cancer screening device with neural network classification for low-resource communities. PloS one, 13(12), p.e0207493.

[20] Ariji, Y., Fukuda, M., Kise, Y., Nozawa, M., Yanashita, Y., Fujita, H., Katsumata, A. and Ariji, E., 2019. Contrast-enhanced computed tomography image assessment of cervical lymph node metastasis in patients with oral cancer by using a deep learning system of artificial intelligence. Oral surgery, oral medicine, oral pathology and oral radiology, 127(5), pp.458-463.

[21] Zhou, Huiyu, Jiahua Wu, and Jianguo Zhang. Digital image processing: part II. Bookboon, 2010.

[22] S. Baro. (2020). Oral Cancer (Lips and Tongue) Images Dataset. Accessed: Oct. 4, 2022. [Online]. Available: https://www.kaggle.com/code/ shivam17299/oral-cancer-lips-and-tongue-images-dataset/data

[23] A. Saber, M. Sakr, O. M. Abo-Seida, A. Keshk, and H. Chen, ''A novel deep-learning model for automatic detection and classification of breast cancer using the transfer-learning technique,'' IEEE Access, vol. 9, pp. 71194–71209, 2021.

[24] J. Rashid, M. Ishfaq, G. Ali, M. R. Saeed, M. Hussain, T. Alkhalifah, F. Alturise, and N. Samand, ''Skin cancer disease detection using transfer learning technique,'' Appl. Sci., vol. 12, no. 11, p. 5714, Jun. 2022

ISSN: 1311-1728 (printed version); ISSN: 1314-8060 (on-line version)

[25] Rani, Pooja, et al. "PCA-DNN: A Novel Deep Neural Network Oriented System for Breast Cancer Classification." EAI Endorsed Transactions on Pervasive Health and Technology 9 (2023).